2024 6th International Conference on Communications, Signal Processing, and their Applications (ICCSPA) | 979-8-3503-8481-9/24/$31.00 ©2024 IEEE | DOI: 10.1109/ICCSPA61559.2024.10794377

GA-CRSK: Gradient Ascent Chirp Rate Shift Keying for High Data-Rate LoRa Communications

Sangwon Shin and Mehmet C. Vuran
Cyber-Physical Networking Lab, School of Computing
University of Nebraska-Lincoln, Lincoln, Nebraska, USA
sshin11@unl.edu, mcv@unl.edu

***Abstract*—The exponential increase in the number of Internet of Things (IoT) devices requires efficient and scalable communication solutions for Low Power Wide Area Networks (LPWANs), including the Long Range (LoRa) standard. LoRa leverages chirp spread spectrum (CSS) modulation to increase coverage at the cost of throughput, preventing the implementation of new IoT applications with higher data rate requirements. Recently, several improvements to CSS modulation have been developed, including a new class of solutions called chirp rate shift keying (CRSK). CRSK solutions incorporate multiple chirp rates within the modulation space to increase the number of bits that could be modulated in a chirp symbol, increasing spectral efficiency. However, the exponential increase in search space for demodulation for each additional bit in CRSK limits throughput improvements over CSS. This paper first generalizes the CRSK demodulation process through discrete chirp Fourier transform (DCFT) techniques to expose the chirp-specific characteristics of the search space. Accordingly, Gradient Ascent Chirp Rate Shift Keying (GA-CRSK) is introduced by utilizing a gradient ascent algorithm and a novel initialization process to drastically accelerate the demodulation speed. GA-CRSK reduces the search iterations by up to 97.16% compared to existing CRSK solutions. Extensive comparative evaluations with state-of-the-art CSS variants show that GA-CRSK improves LoRa throughput by 99.8%, outperforming existing CRSK approaches by 39.4%. To the best of our knowledge, GA-CRSK is the fastest CSS modulation scheme so far.**

***Index Terms*—Low Power Wide Area Networks (LPWAN), Chirp Spread Spectrum (CSS), Long-Range (LoRa) communications, wireless communications**

I. Introduction

The rapid rise of the Internet of Things (IoT) requires communication technologies that can efficiently support a comprehensive set of large-scale verticals [1]. Generally, a trade-off between range and data rate is struck to meet such needs. Accordingly, low power wide area networks (LPWANs) with high energy efficiency are utilized [2]. Among several LPWAN technologies, Long Range (LoRa) is one of the rapidly adopted technologies. LoRa enables connectivity of a massive number of IoT devices, providing an extended range of communication with minimum energy consumption [3]. The physical layer (PHY) of LoRa has gained considerable attention recently with the modifications on the LoRa PHY and MAC schemes [1] [4]. However, LoRa has an explicit low data rate limitation, which does not support applications with high data rate requirements [1]. To overcome such limitations, recent approaches focus on using a multipath channel [5], utilizing Multi-Input Multi-Output (MIMO) [6], or modifying the LoRa modulation scheme [7]–[9]. However, despite their promising increase in throughput, most proposed methods sacrifice the benefits of LoRa, such as energy efficiency and range.

Modifying the modulation scheme in LoRa, known as Chirp Spread Spectrum (CSS), can improve throughput and enhance the effectiveness of LPWAN communication. So far, a few studies have focused on improving CSS modulation to achieve this goal. For instance, Interleaved Chirp Spreading LoRa (ICS-LoRa) [7] increases throughput by introducing sub-intervals, enabling the transmission of more chirps within a single symbol duration. Recently, a family of solutions, which we refer to as Chirp Rate Shift Keying (CRSK), has been developed following similar enhancements to CSS modulation by varying the chirp rate among symbols and using chirp rate as an additional dimension for modulation [10]–[14]. As an example of the CRSK family, Discrete Chirp Rate Keying CSS (DCRK-CSS) [10] enhances throughput by employing multiple chirp rates to modulate extra bits. DCRK-CSS has been demonstrated to provide improved performance with increased throughput and lower error metrics compared to other LoRa enhancements [10].

Despite recent improvements, existing solutions still suffer from limited throughput improvement. For example, DCRK-CSS is shown with only a three-bit improvement over conventional LoRa, leading to only a 50% throughput improvement. As we show in this paper, the main limitation pertains to the increasing complexity of demodulating CRSK signals. These limitations stem from the exponential increase in search space with each addition bit, which is inherent to the exhaustive maximum likelihood search method.

In this paper, we introduce Gradient Ascent Chirp-Rate Shift Keying (GA-CRSK) to enhance the throughput of LoRa communications. GA-CRSK expands the modulation space by incorporating the chirp rate as an additional dimension to increase the number of bits within a chirp symbol. Consequently, the gradient-based search utilizes a greater number of chirp rates to encode data, providing flexibility and achieving higher throughput. The contributions of the paper are as follows:

- We streamline and generalize the demodulation process of chirp-rate shift keying (CRSK) and conduct an in-

979-8-3503-8481-9/24/$31.00 ©2024 IEEE
Authorized licensed use limited to: University of Nebraska - Lincoln. Downloaded on December 29,2024 at 03:14:00 UTC from IEEE Xplore. Restrictions apply.

depth search space analysis for the maximum likelihood estimation. This analysis unveils the distinctive properties of chirp signals that permit the application of novel gradient-based search techniques, enabling swift CRSK demodulation.
- We integrate a gradient ascent-based estimation method along with a novel initialization technique into the demodulation process. The rapid estimation of chirp rate and initial frequency constitutes a major contribution of this paper, significantly enhancing the spectral efficiency of CSS-based modulation.
- We provide a comprehensive theoretical analysis of GA-CRSK performance and conduct comparative evaluations against an extensive set of state-of-the-art CSS solutions. The evaluations demonstrate that **GA-CRSK improves LoRa throughput by more than** 99.8%. Compared to the state-of-the-art CRSK solutions, GA-CRSK provides a 39.4% higher throughput with a 97.16% reduction in convergence time.

To the best of our knowledge, *GA-CRSK is the fastest CSS modulation scheme*, with a promise to lessen the trade-off between throughput and range. GA-CRSK can significantly extend the use of LPWAN technologies by supporting applications that demand high data rates, extensive connectivity, and low energy consumption.

The rest of this paper is organized as follows: The related work is discussed in Section II. The background of CSS modulation, including the recent family of CRSK solutions, is provided in Section III. The CRSK demodulation process is streamlined and generalized in Section IV. Accordingly, the methods and details of GA-CRSK are discussed. GA-CRSK performance is analyzed in Section V with a comparison to state-of-the-art CSS-based solutions. We conclude the paper in Section VI.

II. Related Work

CSS modulation facilitates long-range communication while maintaining low power consumption, offering substantial benefits for various sensor-based networks including the IoT [1], [15]. However, achieving such long-range communication comes with a trade-off in throughput. This limitation restricts the suitability of CSS-based solutions for applications that demand higher throughput (i.e., *advanced* IoT applications). Therefore, recent research on LoRa and CSS modulation has focused on improving the throughput [3]. To this end, three main approaches are observed to enhance the throughput of CSS modulation: parallel transmission, tagging, and modifications on modulation techniques, as we discuss next.

A. Parallel Transmission and Tagging

Parallel transmission and multi-channel transmissions are introduced to boost the data rate of LoRa networks. These methods increase network density without modifying the underlying modulation technique [16]–[18].

Recently, additional computational devices called tags have been utilized with LoRa [19]–[21]. Tags allow multiple LoRa signals to be sent simultaneously with or without modification to the chirp.

However, parallel transmission and tagging-based solutions require extra hardware or MIMO capability, increasing cost, a major benefit of LoRa [1]. Therefore, improving the physical layer of LoRa or CSS modulation is a practical and realistic solution to increase throughput. Compared to parallel transmission and tagging-based methods, GA-CRSK does not require extra hardware, and the cost impact of GA-CRSK is minimal. Furthermore, these solutions are orthogonal to GA-CRSK and can be adopted to improve the network throughput further when hardware costs are justified.

B. Physical Layer Modifications

Several modifications to the CSS modulation have been developed recently to improve its throughput. In [7], Interleaved Chirp Spreading (ICS-LoRa) subdivides the signal by composing the sample into four sub-intervals. This allows one more bit to be modulated compared to the conventional LoRa. Further improvements over ICS-LoRa include the hybrid method in [22], which uses both regular LoRa signals and interleaved signals in the same window. This improves the BER performance while allowing 1 more bit to be modulated compared to LoRa. Moreover, in [23], ICS is combined with slope shift keying (SSK) in [8]. SSK uses a down chirp to modulate the data along with an up chirp. SSK-ICS utilizes this concept by combining up chirp, down chirp, ICS, and SSK together. This allows 2 more bits than CSS to be modulated in a single chirp symbol. In addition to ICS and SSK variations, another approach is to modulate data on both imaginary and real planes by sending each signal on both sine and cosine waves together. More specifically, In-phase Quadrature CSS (IQ-CSS) [9] divides sine and cosine waves to modulate the data, which allows to have 1 extra bits compared to conventional CSS.

Recently, a new family of CSS-variants has been introduced called Chirp Rate Shift Keying (CRSK) [10]–[12], [14]. These approaches leverage multiple chirp rates to be included in the modulation process, providing enhanced capabilities such as increased throughput and robustness against Doppler shift. For example, Discrete Chirp Rate Keying CSS (DCRK-CSS) leverages CRSK to allow 3 additional bits compared to conventional CSS [10]. Within the context of radar and satellite communication, CRSK is utilized in Binary Chirp-Rate Modulation (BCRM) [11] and Multicarrier-Multiple Chirp Rate Shift Keying (MC-MCrSK) [14] to increase robustness against Doppler shift. A similar approach is adopted in Folded Chirp Rate Shift Keying (FCrSK) [12].

Despite the potential of these modulation techniques to modulate additional bits, a significant limitation exists because of the increased complexity of demodulation. In the case of DCRK-CSS, the limitation is made due to the slow demodulation time caused by exhaustive search in maximum likelihood estimation. As shown in Section II, GA-CRSK improves throughput by significantly reducing the number of iterations required for demodulation. To the best of our

Authorized licensed use limited to: University of Nebraska - Lincoln. Downloaded on December 29,2024 at 03:14:00 UTC from IEEE Xplore. Restrictions apply.

knowledge, **GA-CRSK results in the highest throughput** compared to the state of the art.

III. Background

A. CSS Modulation

CSS modulates the signal by spreading energy in frequency linearly within a given bandwidth, B (Hz), over a chirp duration, T_s. CSS modulation defines an initial frequency based on the data symbol. Given a bandwidth, B, in CSS, the spreading factor (SF) is used to define the chirp rate ($\alpha = B^2/2^{SF}$) and the number of bits per symbol ($N = SF$). Based on the data symbol, $\mathbf{b} \in \{0,1\}^{SF}$, the initial frequency index is [9]:

$$k = \sum_{i=0}^{SF-1} 2^i [\mathbf{b}]_\mathbf{i}. \tag{1}$$

where $[\mathbf{b}]_\mathbf{i}$ is the ith bit of $\mathbf{b}$. Then, the data symbols can be represented as integer values from the set of $\mathbb{K} = \{0, 1, ..., 2^N - 1\}$. The transmitted CSS modulated signal can be represented as [24]

$$s_k(t) = \sqrt{\frac{2E_s}{T_s}} exp\left[j2\pi\left(f_k t + (\alpha/2)t^2\right)\right], \tag{2}$$

where E_s and T_s are symbol energy and duration, respectively, f_k is the initial frequency of the kth signal in the constellation and α is the chirp rate[1].

B. CSS Demodulation

A CSS signal is demodulated using Maximum Likelihood (ML) estimation [2]. The received chirp signal, r(t), can be represented as

$$r(t) = s(t) + n(t), \tag{3}$$

where $n(t)$ represents the additive white Gaussian noise (AWGN) with zero mean and a variance of σ^2. The received signals are then demodulated by dechirping the signal by multiplying a down chirp as [24]

$$y(t) = r(t) * exp\left[-j\pi\alpha t^2\right], \tag{4}$$

With a dechirped signal, computing Fast Fourier Transform (FFT) yields a maximum amplitude at a specific initial frequency index, which is used to demodulate the signal as [9]

$$\hat{k} = \underset{k \in \mathbb{K}}{\operatorname{argmax}} \{FFT[y(t)]\}, \tag{5}$$

where $\hat{k}$ represents the recovered data symbol through ML estimation. The characteristics of a linear chirp and the details of CSS modulation in LoRa are available in [26].

C. Chirp Rate Shift Keying

The number of bits, N, modulated by a single CSS symbol depends on the number of distinct initial frequency values determined by SF. This approach provides a single dimension (i.e., initial frequencies) upon which bits could be modulated. A new family of modulation schemes [10], [12], [13] utilize the chirp rate, α, as the second dimension of modulation.

[1]We slightly abuse the notation in (2) for brevity. In practice, the frequency of the chirp is modulo bandwidth as in (8) in [25].

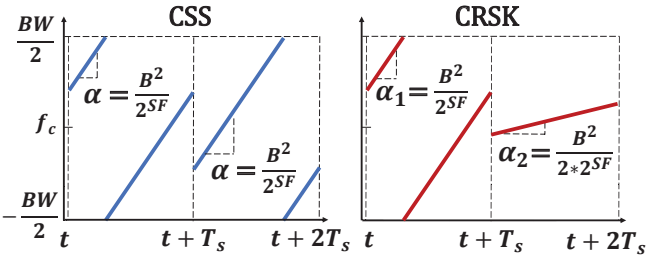

Fig. 1 Difference between CSS chirps and CRSK chirps.

While various names are used, we will refer to this family as Chirp-rate Shift Keying (CRSK). In Fig. 1, the differences between two consecutive symbols of conventional CSS (left) are compared to those of CRSK (right). CRSK solutions modulate the data by using the initial frequency value as well as the chirp rate of the chirp. The additional modulation dimension of the chirp rate increases the number of bits that a single chirp could represent. Since discrete chirps are orthogonal, this approach increases spectral efficiency.

While conventional LoRa modulates SF bits per symbol, CRSK[2] includes CR extra bits to modulate $N = SF + CR$ bits per symbol by incorporating 2^{CR} chirp rates. Accordingly, CRSK can transmit $SF+CR$ bits during the same chirp duration where CSS transmits SF bits. Without loss of generality, for CSRK, consider the binary message $\mathbf{m} = [\mathbf{c}|\mathbf{b}]$, which is a concatenation of $\mathbf{c} \in \{0,1\}^{CR}$ and $\mathbf{b} \in \{0,1\}^{SF}$ modulated in the chirp rate and initial frequency dimensions, respectively. Then,

$$k = \sum_{i=0}^{SF-1} 2^i [\mathbf{b}]_\mathbf{i}, \quad l = \sum_{i=0}^{CR-1} 2^i [\mathbf{c}]_\mathbf{i}, \tag{6}$$

where k and l are the initial frequency and chirp rate indices, respectively. Accordingly, the transmitted CRSK signal is given by

$$s_{k,l}(t) = \sqrt{\frac{2E_s}{T_s}} exp\left[j2\pi\left(f_k t + (\alpha_l/2)t^2\right)\right], \tag{7}$$

where

$$\alpha_l = \frac{B^2}{l \cdot 2^{SF}}. \tag{8}$$

To demodulate the CRSK-modulated data, it is necessary to determine both the chirp rate and initial frequency indices of the received chirp. Existing CRSK approaches demodulate the signal by dechirping and applying FFT to the received signal for each possible chirp rate, followed by a maximum likelihood estimation [10]. Due to the binary exponential increase in the number of chirp rates required for each additional modulated bit, the exhaustive search for ML estimation significantly limits the throughput improvement by CRSK approaches.

[2]Due to the slight variations in the CRSK family [10], [12], [13], we focus on [10] for background specifics.

Authorized licensed use limited to: University of Nebraska - Lincoln. Downloaded on December 29,2024 at 03:14:00 UTC from IEEE Xplore. Restrictions apply.

IV. Gradient Ascent Chirp-rate Shift Keying

The main challenge with CRSK solutions is the exponential increase in search space for demodulation as the additional number of bits, CR, increases, as we show in Section V. This limits the number of bits that could be added in the chirp-rate dimension. As a result, the throughput improvement of CRSK solutions is limited. For example, in [10], $CR \leq 3$. To alleviate this limitation, we first generalize the CRSK demodulation process and analyze the chirp-signal-specific characteristics of the search space. Then, we devise a novel GA-CRSK demodulation solution that drastically reduces demodulation time.

A. CRSK Demodulation Search Space

Assume that a signal is transmitted with initial frequency and chirp rate indices of k^* and l^*, respectively. CRSK demodulation aims to estimate the initial frequency, f_{k^*}, and chirp rate, α_{l^*}, parameters of the transmitted signal. We know from conventional CSS that, if α_{l^*} is known, then f_{k^*} could be estimated by downchirping the received signal with a chirp rate of $-\alpha_{l^*}$ and taking the FFT, which is maximized at f_{k^*}. However, in CRSK, α_{l^*} is not known. Instead, existing approaches use all possible values of α_l to dechirp the signal in multiple parallel channels followed by FFTs [12]. Then, the set of values are maximized at (f_{k^*}, α_{l^*}) in this two dimensional search space. Next, we analyze this search space for a more efficient maximization solution.

Assuming the sampled, discrete version of $s_{(k^*,l^*)}(t)$ in (7) as $s_{(k^*,l^*)}[n]$, the demodulation process could be generalized through Discrete Chirp Fourier Transform (DCFT) [27]. In general, DCFT of $s_{(k^*,l^*)}[n]$ is defined as [27]:

$$S_c(f_k, \alpha_l) = \frac{1}{\sqrt{N}} \sum_{n=0}^{N-1} s_{(k^*,l^*)}[n] \cdot exp\left(-j\pi\alpha_l n^2/N\right) \cdot exp\left(-2j\pi f_k n/N\right), \tag{9}$$

where $k \in [0, 2^{SF}]$, $l \in [0, 2^{CR}]$. Practically, $S_c(f_k, \alpha_l)$ can be calculated by taking 2^{SF}-point FFT of the dechirped signals for each α_l. An example $S_c(f_k, \alpha_l)$ surface with $SF = 12$, $CR = 5$, $k^* = 1852$, and $l^* = 11$ is shown in Fig. 2. Now, we analyze the chirp-specific properties of this search space.

Two main properties of the S_c surface can be observed in Fig. 2. First, the function maximum occurs at (f_{k^*}, α_{l^*}). Moreover, the rate of increase in amplitude is more drastic in the frequency dimension compared to the gradual increase and decrease in the chirp rate dimension around the target f_{k^*}.

To further explore the chirp-specific properties of S_c, $s_{(k^*,l^*)}[n]$ can be plugged in to (9) to yield:

$$S_c(f_k, \alpha_l) = \sqrt{\frac{2E_s}{NT_s}} \sum_{n=0}^{N-1} exp\left(j\pi(\alpha_{l^*} - \alpha_l)n^2/N\right) \cdot exp\left(2j\pi(f_{k^*} - f_k)n/N\right). \tag{10}$$

When, $\alpha_l = \alpha_{l^*}$, the DCFT process reduces to conventional CSS modulation and the function is an impulse function at $f_k = f_{k^*}$. However, when $\alpha_l \neq \alpha_{l^*}$, the signal is dechirped with a mismatched chirp rate. This results in a residual phase of $(\alpha_{l^*} - \alpha_l)n^2/2$. This property can be observed in the zoomed-in inset in Fig. 2, depicting a magnified top-view of the surface around the maximum. The residual quadratic phase causes the instantaneous frequency to correspond to different frequency indices, k. Accordingly, **the energy of the signal is spread proportional to the difference between α_{l^*} and α_l.** Importantly, the amplitude of S_c is maximized for $\alpha_{l^*} = \alpha_l$.

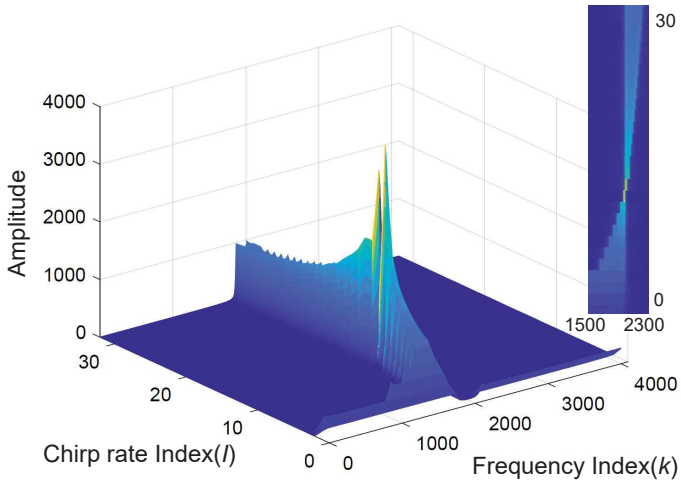

Fig. 2 Discrete Chirp Fourier Transform (DCFT) of GA-CRSK waveform.

Applying maximum likelihood estimation to the S_c function is adopted in the literature [10]. However, searching for the maximum value in a function, where the size grows exponentially with the extra modulating bits, involves an extensive search iteration process. For example, the search space in DCRK-CSS grows from $32,768$ elements for $CR = 3$ to $524,288$ elements for $CR = 7$, as shown in Section V. As a result, in DCRK-CSS, $CR \leq 3$ because of the exhaustive search method used in estimation.

To address the limitations of CRSK approaches, we leverage the unique properties of the search space and develop Gradient Ascent Chirp Rate Shift Keying, which utilizes gradient-based estimation techniques commonly used in machine learning. Using gradient ascent, the maximum point of the non-convex function can be found efficiently [28], as we describe next.

B. GA-CRSK Demodulation

The main contribution of this paper is a novel demodulation algorithm for GA-CRSK using the DCFT formalization above. To this end, we leverage a gradient ascent approach to maximize the two-dimensional DCFT function and estimate the initial frequency and the chirp rate of the received signal. To address the initialization challenge in gradient-based approaches, we devise a novel initialization solution by exploiting the unique structure of the DCFT of a chirp signal. Accordingly, the chirp can be demodulated to yield the original message $\hat{\mathbf{m}} = [\hat{\mathbf{c}}|\hat{\mathbf{b}}]$.

1) Gradient Ascent-based Estimation

Gradient-based search has been commonly used in machine learning to find the local minimum/maximum of a differentiable function by minimizing the loss function of the training

Authorized licensed use limited to: University of Nebraska - Lincoln. Downloaded on December 29,2024 at 03:14:00 UTC from IEEE Xplore. Restrictions apply.

model [29]. However, there is only a handful of work utilizing gradient-based search in wireless communication [30], [31] due to the requirement of the gradient [32]. To the best of our knowledge, this is the first approach utilizing gradient-based estimation as a CSS demodulation technique.

In GA-CRSK, DCFT produces a non-convex function, and our objective is to find the maximum using gradient ascent techniques. The effectiveness of gradient ascent in estimating ML of a two-dimensional non-convex function has been demonstrated for its ability to reduce the number of required search iterations. This efficiency is derived from leveraging minimum error probability, driven by closed-form analytics [33]. Therefore, gradient-based estimation on a DCFT function can reduce the search space with minimum impact in error.

Gradient ascent iteratively adjusts parameters towards the function's steepest increasing value [33]. To this end, the gradient of the function is leveraged, and the step size is updated to adjust the search direction to a greater value. For S_c surface, search point updates through gradient ascent can be represented as:

$$(f_k, \alpha_l) = (f_k, \alpha_l) + \phi \nabla S_c(f_k, \alpha_l), \tag{11}$$

where ϕ is the step size, and $\nabla S_c(f_k, \alpha_l)$ is the gradient of the current iteration of the DCFT function. This can be represented separately as

$$f_k = f_k + \phi \frac{\partial S_c}{\partial f_k}, \quad \text{and} \quad \alpha_l = \alpha_l + \phi \frac{\partial S_c}{\partial \alpha_l}, \tag{12}$$

where $\partial S_c / \partial f_k$ and $\partial S_c / \partial \alpha_l$ indicate the slope of S_c for f_k and α_l, respectively. For the maximum value found by gradient ascent, there is a possibility that the discovered value is the local maxima instead of the global maximum [34]. To avoid the local maxima problem of gradient ascent, it is possible to verify if the discovered maximum is the global or local maximum using the characteristics of DCFT as follows.

In GA-CRSK, the accuracy of the chirp rate for dechirping determines a singular maximum amplitude within the DCFT function, as shown in (10). The amplitude of the DCFT function decreases proportionally with deviations from the correct chirp rate. Therefore, for a given (f_k, α_l), if neighboring amplitudes exceed the current value, then (f_k, α_l) cannot be a global maximum. GA-CRSK addresses this by using gradient ascent to move to adjacent points with higher amplitudes, iteratively refining its position on the surface. This method ensures that GA-CRSK effectively navigates the DCFT function to reach the global maximum.

2) Frequency-Index-First Initialization

Conventional gradient ascent methodologies suffer from the lack of a well-defined initialization process [28]. We introduce a novel Frequency-index-first (FIF) initialization approach to address this challenge, further reducing the search space [35]. The main idea of FIF initialization stems from the observation that the DCFT function increases and decreases more drastically across the frequency index dimension (Fig. 2). Accordingly, the goal is to initialize gradient ascent close to f_{k^*}. FIF involves segmenting the search space to identify a suitable initialization point. To this end, an empirical threshold, S_{th}, is identified. Without loss of generality, FIF first calculates $S_c^{max}(\alpha_0) = \max(\{S_c(f_k, \alpha_0), \forall k\})$ and compares this value with S_{th}. If no amplitude surpasses S_{th}, the function evaluation proceeds to the midpoint of the chirp index range (i.e., $(SF-1)/2$), and so on. This recursive bisection continues until an initial point above S_{th} suitable for gradient ascent is identified.

In contrast to random initialization methods, this tailored approach significantly reduces iteration requirements by focusing the search on areas with substantial amplitude. Consequently, the FIF method accelerates convergence within the extensive parameter space. The pseudo-code of the GA-CRSK demodulation algorithm is available in [26].

V. Performance Evaluations

We evaluate the performance of GA-CRSK through both theoretical and simulation-based analysis. The results are compared to the following comparison set: LoRa, IQ-CSS [9], ICS-LoRa [7], and DCRK-CSS [10].

A. Theoretical Analysis

In GA-CRSK, the coherent detector utilizes the demodulation solution in Section IV-B to estimate the initial frequency, $\hat{f}_k$ and chirp rate, $\hat{\alpha_l}$. Since we leverage existing LoRa waveforms, each symbol carries an orthogonal relationship [36]. Applying orthogonal approximation at the underlying basis signals [37], each GA-CRSK chirp can contain up to 2^{SF+CR} basis signals. Then, the cross-correlation between 2^{SF+CR} possible GA-CRSK basis signals can be described as:

$$R_{k,l} = \sum_{n=0}^{2^{SF+CR}-1} r[n] * s_{\hat{k},\hat{l}}[n]^* \tag{13}$$

$$= \begin{cases} \sqrt{E_s} + \eta & \hat{k} = k^* \text{ and } \hat{l} = l^* \\ \eta & otherwise \end{cases}, \tag{14}$$

where $r[n]$ is the received GA-CRSK signal from AWGN channel, $s_{k,l}[n]^*$ is a complex conjugate of the basis function, $s_{k,l}[n]$, E_s is the energy per symbol with target symbol indices of k^* and l^*. η is a complex Gaussian random variable with zero mean and variance σ^2, which is independent and identically distributed across the index pairs.

Defining $\rho = |\eta|$ as the magnitude of the complex noise envelope and η as a complex zero-mean Gaussian noise process, then ρ depicts a Rayleigh distributed random variable. The probability of symbol error rate can be described as:

$$P_{e|m,p} = Pr\left[\rho > \beta_{k^*,l^*}\right] \tag{15}$$

where $\beta_{k^*,l^*} = |\sqrt{E_s} + \eta|$ and follows a Rician distribution with a shape parameter of $\kappa_\beta = E_s/2\sigma^2 = E_s/N_0$. Let $\hat{\rho}$ depict an identically distributed Rayleigh random variable from the maximum of $2^{SF+CR} - 1$. Then CDF of $\hat{\rho}$ is

$$F_{\rho_k(\rho)} = \left[1 - exp\left(-\rho^2/2\sigma^2\right)\right]^{2^{SF+CR}-1}, \tag{16}$$

Authorized licensed use limited to: University of Nebraska - Lincoln. Downloaded on December 29,2024 at 03:14:00 UTC from IEEE Xplore. Restrictions apply.

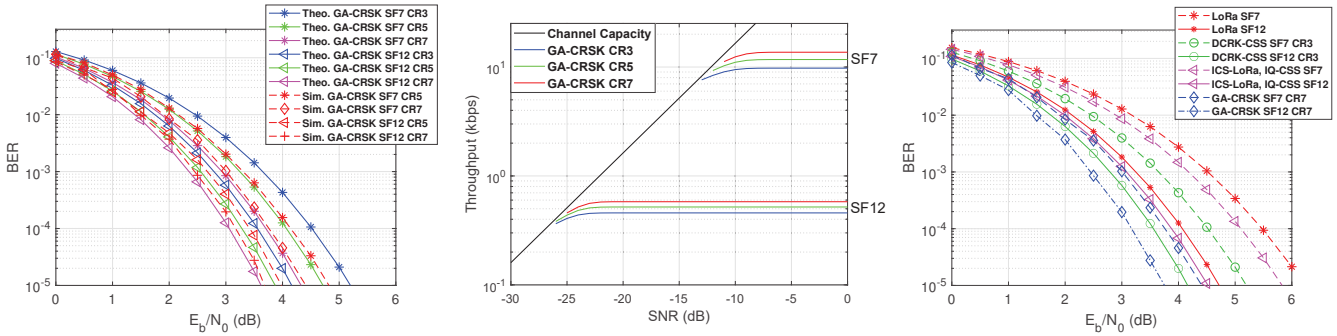

(a) BER vs. Eb/No for GA-CRSK (b) Throughput of GA-CRSK (c) BER vs. Eb/No for comparison set.

Fig. 3: Performance of comparison set and GA-CRSK for different SF and CR configurations.

finally, with (15) and (16), the average bit error probability P_b for GA-CRSK can be described as

$$P_b = 0.5 * \int_0^\infty \left\{1 - \left[1 - exp\left(-\rho^2/2\sigma^2\right)\right]^{2^{SF+CR}-1}\right\} * f_\beta(\beta) d\beta, \tag{17}$$

where $f_\beta(\beta)$ is a probability density function (PDF) for the Rician Distributed value of β as

$$f_\beta(\beta) = \frac{\beta}{\sigma^2} exp\left(-\frac{\beta^2 + E_s}{2\sigma^2} I_0\left(\frac{\beta E_s}{\sigma^2}\right)\right), \tag{18}$$

and I_0 is the modified Bessel Function of the first kind with order zero. To derive each bit error probability with Signal-to-noise ratio (SNR), SNR for GA-CRSK can be defined as:

$$SNR = \frac{E_s/T_s}{N_0 * BW} = \frac{E_s}{N_0 * 2^{SF}}. \tag{19}$$

where E_s can be defined using energy per bit (E_b) as follows:

$$E_s = \frac{E_b * (SF + CR)}{2^{SF}}, \tag{20}$$

GA-CRSK is implemented in MATLAB and the BER performance is evaluated with AWGN channel using Monte Carlo simulations. In Fig. 3a, the theoretical and simulated BER are shown, with less than 0.3 dB difference between the simulated and theoretical results. Next, we evaluate GA-CRSK performance under different combinations of SF and CR values.

B. GA-CRSK Performance Results

In Fig. 3a, the bit error rate (BER) performance is depicted with respect to the energy per bit (E_b/N_o). For a given BER, performance increases by less than 0.4 dB for each 2 bit increment of $SF + CR$. Note that the relationship shown in (20) also increases the energy requirements to maintain the same BER as SF gets lower.

Next, we analyze the effective throughput. For GA-CRSK, the effective throughput (bps) is given as:

$$\rho = \frac{(SF + CR) * BW}{2^{SF}}(1 - BER). \tag{21}$$

For a BER requirement of 10^{-3}, the maximum achievable throughput for each configuration is shown in Fig. 3b. For $SF = 7$, GA-CRSK throughput is 9.8 kbps, 11.7 kbps, and 13.7 kbps for CR values of $3, 5$, and 7 respectively. For $SF = 12$, the throughput values are 457 bps, 518 bps, and 579 bps, respectively. It can be observed that a higher CR value requires in a higher minimum SNR to reach the maximum throughput in a given configuration. For $SF = 7$, for each increment of CR value from 3, 5, to 7; a 1 dB increment in minimum SNR is needed to reach the maximum throughput. For $SF = 12$, this required minimum SNR increment is less than 0.5 dB for each increment in CR from 3, 5, and 7. The results show that the configuration of SF and CR in GA-CRSK strikes a balance betwee BER and throughput. Therefore, GA-CRSK allows flexibility in controlling communication quality and throughput. This is achieved by selecting SF and CR based on the channel quality and application needs. Next, the performance of GA-CRSK is compared with existing CSS-based modulation schemes.

C. Comparative Evaluations

The performance of GA-CRSK is compared to LoRa, IQ-CSS [9], ICS-LoRa [7], and DCRK-CSS [10]. For IQ-CSS and DCRK-CSS, the theoretical performance has been calculated based on the analytical model in [36], and ICS-LoRa performance is calculated based on the analytical model shown in [7]. The performance of each modulation scheme is evaluated under AWGN channels in terms of (i) bit error ratio (BER) as a function of energy per bit to noise ratio (E_b/N_0) and (ii) achievable throughput as a function of SNR. The parameters used for comparison between GA-CRSK and other CSS-based modulations are chosen based on U.S. standards of LoRa operating in industrial, scientific, and medical (ISM) bands [38] with bandwidths of 125 kHz and 500 kHz.

In Fig. 3c, the BER is shown for $SF = 7$ and $SF = 12$ to evaluate the LoRa, IQ-CSS, DCRK-CSS, ICS-LoRa, and GA-CRSK. In addition, for DCRK-CSS ($CR = 3$) and GA-CRSK ($CR = 7$), the highest explored settings are chosen. For a given BER requirement, the CSS-variants improve Eb/No requirement compared to LoRa in the order of ICS-LoRa, DCRK-CSS, and GA-CRSK since each modulation scheme

Authorized licensed use limited to: University of Nebraska - Lincoln. Downloaded on December 29,2024 at 03:14:00 UTC from IEEE Xplore. Restrictions apply.

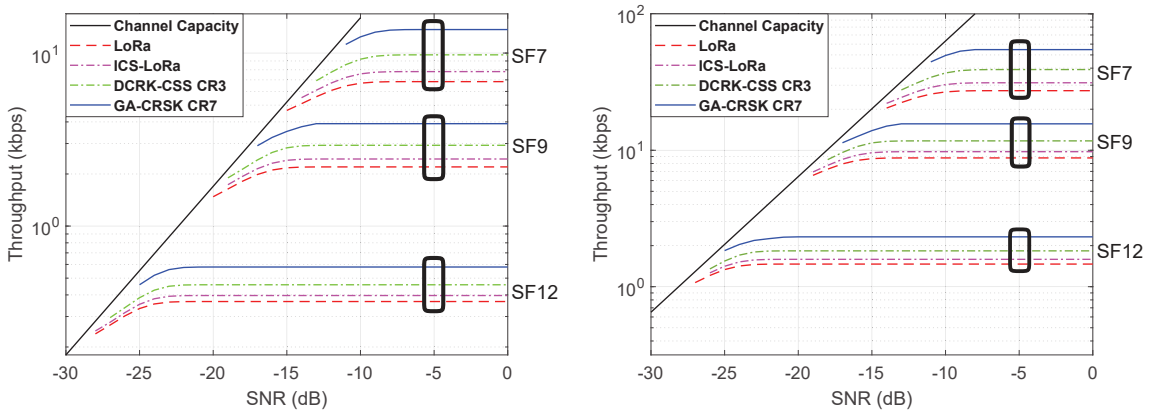

(a) BW=125 kHz

(b) BW=500 kHz

Fig. 4: Throughput comparison.

has 3, 5, and 7 extra bits, respectively. Since the energy per bit required to maintain the BER for GA-CRSK with $SF = 12$ $CR = 7$ contains the most amount of bits per symbol compared to other modulation schemes, GA-CRSK shows the highest performance with E_b/N_0 of 3.7 dB.

The achievable throughput of each modulation scheme is shown in Figs. 4 with bandwidths of 125 kHz and 500 kHz for $SF = 7, 9, 12$. **GA-CRSK delivers the highest throughput** in the comparison set. Considering the largest coverage configuration of 125 kHz and $SF = 12$ (Fig. 4a), GA-CRSK throughput is 58.3% higher than that of LoRa (366 bps vs. 579.8 bps) with $CR = 7$. Similarly, GA-CRSK outperforms ICS-LoRa and DCRK-CSS by 46.1% and 26.7%, respectively. At a bandwidth of 500 kHz, GA-CRSK results in 53.3% higher throughput than LoRa (1.5 kbps vs. 2.3 kbps).

The largest throughput improvement of GA-CRSK is observed with $SF = 7$. With a 125 kHz bandwidth, GA-CRSK is 99.8% faster than LoRa (6.83 kbps vs. 13.67 kbps). At this configuration, GA-CRSK outperforms ICS-LoRa (7.8 kbps) and DCRK-CSS (9.8 kbps) by 75.2% and 39.4%, respectively. With a bandwidth of 500 kHz, **GA-CRSK doubles the throughput of LoRa** (27.3 kbps vs. 54.6 kbps). Note that the increased throughput of GA-CRSK can decrease the number of chirps in each payload, *decreasing transmission time and hence, energy consumption*.

TABLE I: Iterations for Convergence

Parameter	DCRK-CSS	GA-CRSK	Decrease (%)
$SF\,12, CR\,3$	$32,768$	$2,951$	90.99%
$SF\,12, CR\,5$	$131,072$	$11,282$	91.39%
$SF\,12, CR\,7$	$524,288$	$14,873$	97.16%

The throughput improvement in GA-CRSK is achieved through fast demodulation enabled by gradient ascent. In Table I, we compare GA-CRSK to state-of-the-art (DCRK-CSS) in terms of the number of iterations required for convergence for $SF = 12$. At $CR = 3$, GA-CRSK requires 90.99% less number of iterations than DCRK-CSS. The reduction is larger as CR increases. For example, at $CR = 7$, a 97.16% reduction is observed. It is important to note that in [10], CR is limited to 3, and the reason could be observed in Table I. Remarkably, GA-CRSK requires 54.6% less iterations at $CR = 7$ $(14,873)$ than what DCRK-CSS requires at $CR = 3$ $(32,768)$.

Overall, GA-CRSK demonstrates a significant throughput improvement of 99.8% compared to LoRa and a substantial 39.4% increase over the state-of-the-art CRSK modulation scheme. The extensive evaluations reveal that GA-CRSK stands out as the **fastest CSS-variant** yet.

VI. Conclusion

In this paper, we develop Gradient Ascent Chirp Rate Shift Keying (GA-CRSK), which provides the highest throughput compared to state-of-the-art CSS modulation schemes. GA-CRSK improves LoRa throughput by over 99.8% and significantly outperforms CRSK schemes. The novel demodulation approach reduces the number of iterations required for convergence by up to 97.16%. By modulating a larger number of bits per symbol, GA-CRSK can effectively reduce communication duration and energy consumption in IoT networks. As a complete transmission modulation package, GA-CRSK provides coherent demodulation using Discrete Chirp Fourier Transform with stochastic gradient search techniques for a faster maximum likelihood estimation. The extensive theoretical and simulation-based analysis also compares the bit error rate performance of GA-CRSK with the state-of-the-art CSS variants, including LoRa, ICS-LoRa, and DCRK-CSS. As a future work, we aim to further explore combinations of SF and CR to navigate the acceptable range of BER and throughput trade-offs. Moreover, GA-CRSK will be implemented in a Software Defined Radio to evaluate real-world usage and performance capabilities.

Acknowledgment

This research is supported in part by the National Science Foundation (NSF) ECCS-2030272 grant and the Daugherty Water for Food Institute.

Authorized licensed use limited to: University of Nebraska - Lincoln. Downloaded on December 29,2024 at 03:14:00 UTC from IEEE Xplore. Restrictions apply.

REFERENCES

[1] Ferran Adelantado, Xavier Vilajosana, Pere Tuset-Peiro, Borja Martinez, Joan Melia-Segui, and Thomas Watteyne. Understanding the Limits of LoRaWAN. *IEEE Communications Magazine*, 55(9):34–40, 2017.

[2] Brecht Reynders and Sofie Pollin. Chirp spread spectrum as a modulation technique for long range communication. In *2016 Symposium on Communications and Vehicular Technologies (SCVT)*, pages 1–5, 2016.

[3] Juha Petäjäjärvi, Konstantin Mikhaylov, Marko Pettissalo, Janne Janhunen, and Jari Iinatti. Performance of a low-power wide-area network based on LoRa technology: Doppler robustness, scalability, and coverage. *International Journal of Distributed Sensor Networks*, 13(3):1550147717699412, 2017.

[4] Rui Fernandes, Rui Oliveira, Miguel Luís, and Susana Sargento. On the Real Capacity of LoRa Networks: The Impact of Non-Destructive Communications. *IEEE Communications Letters*, 23(12):2437–2441, 2019.

[5] Clément Demeslay, Philippe Rostaing, and Roland Gautier. Theoretical Performance of LoRa System in Multipath and Interference Channels. *IEEE Internet of Things Journal*, 9(9):6830–6843, 2022.

[6] Jae-Mo Kang. MIMO-LoRa for High-Data-Rate IoT: Concept and Precoding Design. *IEEE Internet of Things Journal*, 9(12):10368–10369, 2022.

[7] Tallal Elshabrawy and Joerg Robert. Interleaved Chirp Spreading LoRa-Based Modulation. *IEEE Internet of Things Journal*, 6(2):3855–3863, 2019.

[8] Muhammad Hanif and Ha H. Nguyen. Slope-Shift Keying LoRa-Based Modulation. *IEEE Internet of Things Journal*, 8(1):211–221, 2021.

[9] Ivo Bizon Franco de Almeida, Marwa Chafii, Ahmad Nimr, and Gerhard Fettweis. In-phase and Quadrature Chirp Spread Spectrum for IoT Communications. In *GLOBECOM 2020 - 2020 IEEE Global Communications Conference*, pages 1–6, 2020.

[10] Ivo Bizon Franco de Almeida, Marwa Chafii, Ahmad Nimr, and Gerhard Fettweis. Alternative Chirp Spread Spectrum Techniques for LP-WANs. *IEEE Transactions on Green Communications and Networking*, 5(4):1846–1855, 2021.

[11] Bing Deng, Ran Tao, and Enqing Chen. Anovel method for binary chirp-rate modulation and demodulation. In *2006 8th international Conference on Signal Processing*, volume 3, 2006.

[12] Chao Yang, Mei Wang, Lin Zheng, and Guangpeng Zhou. Folded chirp-rate shift keying modulation for leo satellite iot. *IEEE Access*, 7:99451–99461, 2019.

[13] Yu Liu, Qian Liu, Shuhong Gong, Muyu Hou, and Rui Xu. Chirp-rate shift keying modulation for mechanical antenna based on rotating dipoles. *IEEE Transactions on Antennas and Propagation*, 71(4):2989–2999, 2023.

[14] Cheng En, Lin Xiaoyang, and Yuan Fei. Multiuser underwater acoustic communication based on multicarrier-multiple chirp rate shift keying. In *OCEANS 2014 - TAIPEI*, pages 1–5, 2014.

[15] Jansen C. Liando, Amalinda Gamage, Agustinus W. Tengourtius, and Mo Li. Known and Unknown Facts of LoRa: Experiences from a Large-Scale Measurement Study. *ACM Trans. Sen. Netw.*, 15(2), feb 2019.

[16] Xianjin Xia, Yuanqing Zheng, and Tao Gu. FTrack: Parallel Decoding for LoRa Transmissions. *IEEE/ACM Transactions on Networking*, 28(6):2573–2586, 2020.

[17] Pieter Robyns., Peter Quax., Wim Lamotte., and William Thenaers. A Multi-Channel Software Decoder for the LoRa Modulation Scheme. In *Proceedings of the 3rd International Conference on Internet of Things, Big Data and Security - IoTBDS,*, pages 41–51. INSTICC, SciTePress, 2018.

[18] Yi Yu, Lina Mroueh, Diane Duchemin, Claire Goursaud, Guillaume Vivier, Jean-Marie Gorce, and Michel Terré. Adaptive Multi-Channels Allocation in LoRa Networks. *IEEE Access*, 8:214177–214189, 2020.

[19] Yao Peng, Longfei Shangguan, Yue Hu, Yujie Qian, Xianshang Lin, Xiaojiang Chen, Dingyi Fang, and Kyle Jamieson. PLoRa: A Passive Long-Range Data Network from Ambient LoRa Transmissions. In *Proceedings of the 2018 Conference of the ACM Special Interest Group on Data Communication*, SIGCOMM '18, page 147–160, New York, NY, USA, 2018. Association for Computing Machinery.

[20] Jinyan Jiang, Zhenqiang Xu, Fan Dang, and Jiliang Wang. *Long-Range Ambient LoRa Backscatter with Parallel Decoding*, page 684–696. Association for Computing Machinery, New York, NY, USA, 2021.

[21] Yuxiang Peng, Shiyue He, Yu Zhang, Zhiang Niu, Lixia Xiao, and Tao Jiang. Ambient LoRa Backscatter System With Chirp Interval Modulation. *IEEE Transactions on Wireless Communications*, 22(2):1328–1342, 2023.

[22] Md. Noor-A-Rahim, M. Omar Khyam, Apel Mahmud, Xinde Li, Dirk Pesch, and H. Vincent Poor. Hybrid Chirp Signal Design for Improved Long-Range (LoRa) Communications. *Signals*, 3(1):1–10, 2022.

[23] Aniket Mondal, Muhammad Hanif, and Ha H. Nguyen. SSK-ICS LoRa: A LoRa-Based Modulation Scheme With Constant Envelope and Enhanced Data Rate. *IEEE Communications Letters*, 26(5):1185–1189, 2022.

[24] S. Hengstler, D.P. Kasilingam, and A.H. Costa. A novel chirp modulation spread spectrum technique for multiple access. In *IEEE Seventh International Symposium on Spread Spectrum Techniques and Applications,*, volume 1, pages 73–77 vol.1, 2002.

[25] Yubi Qian, Lu Ma, and Xuwen Liang. Symmetry chirp spread spectrum modulation used in LEO satellite internet of things. *IEEE Communications Letters*, 22(11):2230–2233, 2018.

[26] Sangwon Shin and Mehmet C. Vuran. GA-CRSK: gradient ascent chirp rate shift keying for high data-rate LoRa communications. Technical Report TR-UNL-CSE-2024-0001, University of Nebraska-Lincoln, June 2024. Available at https://http://cse-apps.unl.edu/facdb/publications/TR-UNL-CSE-2024-0001.pdf.

[27] Xiang-gen Xia. Discrete chirp-Fourier transform and its application to chirp rate estimation. *IEEE Transactions on Signal Processing*, 48(11):3122–3133, 2000.

[28] An Liu, Vincent K. N. Lau, and Borna Kananian. Stochastic successive convex approximation for non-convex constrained stochastic optimization. *IEEE Transactions on Signal Processing*, 67(16):4189–4203, 2019.

[29] Kenneth Levenberg. A method for the solution of certain non-linear problems in least squares. *Quarterly of applied mathematics*, 2(2):164–168, 1944.

[30] Ankur Pandey, Pinky Pinky, and Sudhir Kumar. Localization Using Stochastic Gradient Descent Method in a 5G Network. In *2018 15th IEEE India Council International Conference (INDICON)*, pages 1–6, 2018.

[31] Niranjan M Gowda, Sundar Krishnamurthy, and Andrey Belogolovy. Metropolis-Hastings Random Walk along the Gradient Descent Direction for MIMO Detection. In *ICC 2021 - IEEE International Conference on Communications*, pages 1–7, 2021.

[32] Herbert Robbins and Sutton Monro. A Stochastic Approximation Method. *The Annals of Mathematical Statistics*, 22(3):400 – 407, 1951.

[33] A. N'Guessan, I. Geraldo, and B. Hafidi. An Approximation Method for a Maximum Likelihood Equation System and Application to the Analysis of Accidents Data. *Open Journal of Statistics*, 7(1):132–152, 2017.

[34] P.E. Allard and S. Hudon. Gradient descent decoding of binary cyclic codes. In *Proceedings of Canadian Conference on Electrical and Computer Engineering*, pages 253–254 vol.1, 1993.

[35] T. H. Cormen, R. L. Rivest C. E. Leiserson, and C. Stein. *Introduction to Algorithms*. Mass: MIT Press, 2022.

[36] Giuseppe Baruffa and Luca Rugini. Performance of LoRa-Based Schemes and Quadrature Chirp Index Modulation. *IEEE Internet of Things Journal*, 9(10):7759–7772, 2022.

[37] Tallal Elshabrawy and Joerg Robert. Analysis of BER and Coverage Performance of LoRa Modulation under Same Spreading Factor Interference. In *2018 IEEE 29th Annual International Symposium on Personal, Indoor and Mobile Radio Communications (PIMRC)*, pages 1–6, 2018.

[38] LoRa Alliance Technical Committee Regional Parameters Workgroup. LoRaWAN™ 1.0.3 Regional Parameters. Technical report, LoRa Alliance, Inc, 2018.

Authorized licensed use limited to: University of Nebraska - Lincoln. Downloaded on December 29,2024 at 03:14:00 UTC from IEEE Xplore. Restrictions apply.